

Model-Free Error Assessment for Breadth-First Studies, with Applications to Cell-Perturbation Experiments

Jackson Loper

Department of Statistics, University of Michigan

Jeffrey Regier

Department of Statistics, University of Michigan

June 11, 2024

Abstract

With the advent of high-throughput screenings, it has become increasingly common for studies to devote limited resources to estimating many parameters imprecisely rather than to estimating a few parameters well. In these studies, only two or three independent replicates measure each parameter, and therefore it is challenging to assess the variance of these measurements. One solution is to pool variance estimates across different parameters using a parametric model of estimator error. However, such models are difficult to specify correctly, especially in the presence of “batch effects.” In this paper, we propose new model-free methods for assessing and controlling estimator error. Our focus is on type S error, which is of particular importance in many settings. To produce tight confidence intervals without making unrealistic assumptions, we improve on Hoeffding’s bounds for sums of bounded random variables and obtain the tightest possible Chernoff-Cramér bound. Our methods compare favorably with existing practice for high-throughput screenings, such as methods based on the Irreproducible Discovery Rate (IDR) and the Benjamini-Hochberg procedure. Existing practices fail to control error at the nominal level in some cases and are needlessly conservative in others.

Keywords: data splitting, type S error, Hoeffding inequality, estimator error, high-throughput

1 Introduction

Many modern scientific studies devote limited resources to estimating many parameters imprecisely rather than to estimating a few parameters well [Subramanian et al., 2017b, Srivatsan et al., 2020, Schmidt et al., 2022]. We term these studies “breadth-first.”

Breadth-first studies are widely employed to understand complex systems in which the overall behavior is governed by a large number of factors. Gene regulatory networks are one example of such a complex system. Changes in gene expression allow organisms to grow and develop [Wang et al., 2022, Shi et al., 2022] and underlie many disease mechanisms [Yoon et al., 2022, Xie et al., 2022]. Understanding these changes facilitates the development of new treatments [Subramanian et al., 2017b, Srivatsan et al., 2020]. Recent advances in the design of breadth-first CRISPR screens allow unprecedented insight into the causal structure of gene regulatory networks: we can directly alter gene expression in a pool of cells and observe how all other gene expressions change in response [Shifrut et al., 2018, Schmidt et al., 2022]. Previously, such causal networks could be estimated only indirectly by studying correlation structures among observational data, using tools such as the graphical lasso [Chen et al., 2016] and Bayesian latent Gaussian graph mixtures [Wu and Luo, 2022]. However, the estimates from such high-throughput studies are not always reliable [Lim and Pavlidis, 2021]. Thus, there is a pressing need to quantify error in this context.

In this paper, we focus on breadth-first studies where the sign of a parameter (positive or negative) is of central interest. For example, a cell-perturbation screen can be used to estimate whether a particular perturbation in a particular context increases or decreases expression of a particular gene. If an estimator indicates upregulation though the truth is downregulation, or vice-versa, the estimator has committed a sign error, also known as type S error [Gelman and Tuerlinckx, 2000]. It is difficult to use estimators of differential gene

expression if the probability of type S error is large, as the gene control circuits that govern cell behavior are defined in terms of upregulation and downregulation of genes [Davidson, 2001].

How can we assess the number of type S errors in a collection of sign estimates from a breadth-first study? This is the central question that this paper addresses. It is a challenging question because typical study designs do not yield multiple independent measurements of each parameter, and it is difficult to infer variance without independent measurements. Dependencies, which are not easily modeled explicitly, arise from factors such as humidity or technician proficiency, and in breadth-first studies these dependencies have a significant impact on the estimates [Stein et al., 2015]. In some cases, experimentalists can overcome the challenge by relying on prior experience to estimate the magnitude of the measurement noise [Subramanian et al., 2017b, Qiu et al., 2020]. In other cases, parametric error models can be fit to data [Dadaneh et al., 2020]. However, often neither approach captures all the factors that influence experimental measurements, as many of these factors are unobserved and uncontrollable factors.

Performing the same study design multiple times offers one way forward. Given many replicates of the same study design, we can assess how different replicates' estimates vary around the grand mean. This variability around the grand mean may arise from measurement noise or differences in protocol implementation [Mathur and VanderWeele, 2020], but in either case the magnitude of this variability offers some insight into the trustworthiness of the grand mean as an estimate. Conducting many replicates is often prohibitively expensive; for breadth-first cell-perturbation experiments, it is rare to see more than three replicates. With few replicates, precise assessment of each estimate's variance is still challenging; it can only be obtained by making additional assumptions. For example, Zhao

et al. [2020] consider the assumption that all estimates have the same variance. As another example, Li et al. [2011] consider the assumption that the copula of estimates from two replicates can be modeled with a two-component Gaussian mixture model.

We propose a new condition under which a small number of replicates can be used to accurately assess the number of type S errors in a collection of estimates (Section 2). We suppose that the probability that each estimate has the correct sign is at least $1/2$. This probability is considered with respect to all sources of randomness in study implementation—including unobserved ones—such as lab humidity, proficiency of lab technicians, and ambiguities in the study’s protocol. We say that an estimate that satisfies this assumption is “faithful.”

The number of type S errors in the estimates of one replicate can be bounded using another replicate of the study if the estimates of the second replicate are faithful (Section 2.1). We provide intuition for this result here. Suppose that we have one set of sign estimates for a large number of parameters. We then conduct a study, producing new sign estimates for the same parameters. If the expected proportion of sign disagreements between the original estimates and the new estimates is less than β , then, due to the faithfulness assumption, the proportion of sign errors in the original estimates is at most 2β .

We can estimate the expected proportion of sign disagreements, which we term the “sign disagreement rate” (SDR), using the *observed* proportion of sign disagreements between two replicates. We call this observed proportion the “sign disagreement proportion” (SDP). We can obtain a nontrivial confidence interval for our estimate of the SDR as long as the study design includes several independent modules (Section 2.2). For example, consider a cell-perturbation study that tests many different stimuli. For a single stimulus, the expression measurements for different genes may be highly correlated; all measurements are typically

taken from the same pool of cells. On the other hand, suppose that the study is composed of modules that independently investigate different stimuli. In this case, we can partition the parameters of interest (and our estimates of them) by module. Given a partition of our estimates into independent groups, we can obtain nontrivial confidence intervals for the sign disagreement rate using tail bounds on sums of bounded random variables.

To calculate tail bounds on the sums of bounded random variables, we initially used the results of Hoeffding [1963]. However, we found these tail bounds to be so conservative that they are trivial in many cases. For this reason, we have improved Hoeffding’s results. Recall that Hoeffding’s original results include two theorems. His first theorem considers the sum of n independent random variables, each contained in the unit interval. Hoeffding demonstrated a tight upper bound on the moment-generating function of the sum in terms of the expectation of the sum, leading to the tightest possible Chernoff-Cramér bound. Hoeffding’s second theorem considers a sum of independent bounded random variables, where each variable is contained in an interval of different size; it gives an upper bound on the moment-generating function of this sum. However, the upper bound in the second theorem is not tight.

The gap between these two theorems of Hoeffding has persisted since they were originally published. In this paper, we calculate the exact upper bound on the corresponding moment-generating function, leading to the tightest possible Chernoff-Cramér bounds (Section 2.2). This resolves the gap between the two theorems and leads to useful confidence intervals for the sign disagreement rate in practice.

The improved Hoeffding bound enables us to estimate the SDR with confidence. This ability, in turn, enables us to devise the second contribution of this paper: sign error control methods based on SDR (Section 2.4). A “sign error control method” here indicates

a method of using data to select a subset of parameters and estimate the sign of each parameter in the subset, such that the proportion of incorrect sign estimates is typically below a target error level. Our approach to sign error control is as follows. Assume that we are given a collection of estimates for a collection of parameters, together with a scalar confidence score for each estimate. For example, the confidence score for each parameter could be given by the negative p -value for the null hypothesis that the parameter is zero, constructed under a misspecified model. We then construct a sequence of nested subsets of parameters; each particular subset includes all parameters associated with confidence scores greater than a particular threshold. Based on measurements from a second collection of estimates, we then estimate the sign disagreement rate for each subset. Using a submartingale inequality, we can construct a simultaneous $(1 - \alpha)$ confidence region for the sequence of sign disagreement rates associated with this sequence of subsets. We select the largest subset for which the upper bound of the confidence interval is below a user-selected error level. Regardless of how the confidence scores were formed (i.e., even if they were formed using a misspecified model), this subset is guaranteed to control a new variation on false discovery exceedance [Genovese and Wasserman, 2006] that we dub “false sign discovery exceedance.”

Simulations and case studies show the benefits of using the sign disagreement rate to assess and control error (Section 3). Error control methods based on SDR avoid several pitfalls of model-based methods (Section 3.1) and validate existing intuitions among practitioners about the relative merits of two different cell-perturbation study designs (Section 3.2). Error control methods based on the SDR can yield more discoveries than model-based approaches, given a fixed error control target (Section 3.3). The SDP is trivial to compute and the faithfulness assumption is readily explained, offering practitioners a simple model-free

way to think about error in their data.

2 Model-free error assessment through the sign disagreement rate

2.1 The connection between sign disagreement proportions and error proportions

Consider n real-valued parameters of interest, $\theta_1, \dots, \theta_n$. For example, in cell-perturbation studies, a parameter of interest may indicate how a particular gene’s expression changes when a particular population of cells in a particular kind of environment is exposed to a particular stimulus; positive values correspond to upregulation and negative values correspond to downregulation.

For each parameter θ_i , suppose that we have an estimate of its sign $\hat{y}_i \in \{-1, 1\}$. We refer to the vector $\hat{\mathbf{y}}$ as the proposed signs.¹ We seek to assess the proportion of sign errors among the proposed signs. We define this proportion as follows.

Definition 1. The “type S error proportion” of the proposed signs as estimates of the signs of the parameters is $V(\hat{\mathbf{y}}, \boldsymbol{\theta}) = |\{i : \hat{y}_i \neq \text{sign}(\theta_i)\}|/n$.

To estimate the type S error proportion of the proposed signs, suppose that we perform a study obtaining measurements about the vector $\boldsymbol{\theta}$. We assume that the measurements of this study are independent of the proposed signs. For each $i \in \{1, \dots, n\}$, the study

¹Although the parameter may be identically zero, we require each estimate to indicate a direction; we do not permit \hat{y}_i to take the value 0. However, as detailed in Section 2.4, we can use user-supplied confidence scores that quantify uncertainty in each estimate; if no estimate of the sign is available, we can select a sign at random and set this confidence score to zero.

yields an estimate, denoted Y_i , of the sign of θ_i . We refer to the vector $\mathbf{Y} \in \{-1, 1\}^n$ as the validation signs. We thus have two estimates of the sign of each parameter: the proposed sign \hat{y}_i and the validation sign Y_i . We consider the proportion of validation signs that agree with the proposed signs, defined as follows.

Definition 2. The “sign disagreement proportion” between the proposed signs $\hat{\mathbf{y}} \in \{-1, 1\}^n$ and the validation signs $\mathbf{Y} \in \{-1, 1\}^n$ is

$$\text{SDP}(\mathbf{Y}; \hat{\mathbf{y}}) = |\{i : Y_i \neq \hat{y}_i\}|/n.$$

Variability in the SDP arises from two sources: randomness in the proposed signs and randomness in the validation signs.

Our subsequent analysis conditions on the proposed signs, while continuing to treat the validation signs as random. In the same way that conditional permutation tests facilitate model-free hypothesis testing (e.g., [Rosenbaum, 1984]), analyzing this conditional distribution instead of the full joint distribution on proposed signs and validation signs facilitates model-free inferences about the type S error proportion. By denoting the proposed signs with a lowercase $\hat{\mathbf{y}}$ and referring to them in the past tense (“proposed”) while denoting the validation signs with an uppercase \mathbf{Y} , we hope to help the reader keep this conditioning in mind.

We now consider the expected SDP. The expectation is taken with respect to the randomness in the validation signs while the proposed signs are conditioned upon.

Definition 3. The “sign disagreement rate” is $\text{SDR}(\hat{\mathbf{y}}) = \mathbb{E}[\text{SDP}(\mathbf{Y}; \hat{\mathbf{y}})|\hat{\mathbf{y}}]$.

We assume that the validation signs are faithful in the following sense.

Definition 4. A “faithful” validation sign for θ_i is a random variable $Y_i \in \{-1, 1\}$ such that $\mathbb{P}(\text{sign}(\theta_i) = Y_i) \geq 1/2$. More generally, a “ q -faithful” validation sign satisfies $\mathbb{P}(\text{sign}(\theta_i) =$

$Y_i) \geq q$.

The sign disagreement rate based on q -faithful validation signs bounds the type S error proportion by a linear inequality, as the following theorem shows.

Theorem 1. *If $\mathbf{Y} \in \{-1, 1\}^n$ is a vector of q -faithful validation signs for $\boldsymbol{\theta}$, then the type S error proportion is bounded by $V(\hat{\mathbf{y}}, \boldsymbol{\theta}) \leq \text{SDR}(\hat{\mathbf{y}})/q$.*

In a cell-perturbation context, the proposed signs and validation signs can be obtained from multiple replicates of the same study design. Given R replicates, we suggest combining R_p replicates (for example, by averaging estimates) to obtain the proposed signs and combining the other $R - R_p$ replicates to obtain validation signs. There is an asymmetry to this procedure, as there are R choose R_p ways to assign replicates to the two splits, all permissible, yet one must be selected to compute an SDR. One could estimate the SDR for each of the R choose R_p splits, and average the estimates. As the number of replicates grows, this quantity converges to the typical disagreement proportion between sign estimates based on a combination of R_p replicates and sign estimates based on a combination of $R - R_p$ replicates. According to Theorem 1, under an assumption of q -faithfulness, this quantity divided by q asymptotically converges to an upper bound on the mean error proportion committed by a combination of R_p replicates. Alternatively, one could consider a single arbitrary split, as the SDP observed for a particular split can be used to compute a (non-asymptotic) confidence interval for the proportion of sign errors in a collection of proposed signs. In practice, for many studies $R = 2$, in which case $R_p = 1$ is the only viable choice [Shifrut et al., 2018, Schmidt et al., 2022, Srivatsan et al., 2020].

Although low SDR between the proposed signs and the validation signs implies a low type S error proportion in the proposed signs, SDR as high as 1/2 does not imply that the proposed signs contain many errors. This point is demonstrated in the following toy

example, which concerns estimation of a single parameter.

Example 1. Suppose that $\theta \in \mathbb{R}^1$ comprises a single unknown parameter with $\theta > 0$. Suppose further that $\hat{y} = 1$, and therefore the proportion of errors is zero. Now consider a validation sign $Y \in \{-1, 1\}$ with $\mathbb{P}(Y = 1) = 1/2$. This Y is a faithful validation sign because it is correct with probability at least $1/2$. However, the sign disagreement rate is $1/2$ because Y disagrees with \hat{y} with probability $1/2$.

Consequently, the SDR provides a useful upper bound on the proportion of type S errors, though it may not be helpful for setting a lower bound on these errors.

2.2 Estimation of the SDR

To estimate the SDR, we may use the SDP (an unbiased estimator). How shall we quantify our uncertainty about this estimate?

The independence structure of the data provides a means to calculate confidence intervals for the SDR. Let $\{P_1, \dots, P_m\}$ be a partition of the indices of the parameters, $\{1, \dots, n\}$. We refer to each P_i as a module (i.e., we consider a breadth-first study design composed of m modules). For example, in a study that tests the effects of many drugs on many genes, each distinct drug could correspond to one module. For each module i , let $a_i = |P_i|$ denote the total number of parameters investigated by that module, and let X_i denote the number of parameters in that module for which the proposed signs agree with the validation signs, that is,

$$X_i = \sum_{j \in P_i} \mathbb{I}_{Y_j = \hat{y}_j}. \quad (1)$$

Each X_i lies in the set $\{0, 1, \dots, a_i\}$. We assume that X_1, \dots, X_m are conditionally independent given $\hat{\mathbf{y}}$ and θ . Let $S = \sum_i X_i$ and $A = \sum_i a_i$. In these terms, the SDP may be

expressed as $1 - S/A$ and the SDR may be expressed as $1 - \mathbb{E}[S \mid \hat{\mathbf{y}}]/A$. Throughout what follows, we suppress the conditional notation. For example, we may write $\text{SDR} = 1 - \mathbb{E}[S]/A$.

We now construct a one-sided confidence interval on the SDR based on an observation of the SDP, bounding the SDR from above. This interval can provide evidence via Theorem 1 that the type S error proportion is small.

We formulate the problem in terms of hypothesis tests on the value of $\mathbb{E}[S]$. Confidence intervals for the SDR can be obtained by inverting the corresponding hypothesis tests. That is, a valid confidence set for the SDR may be formed by excluding all values c such that the null hypothesis that $1 - \mathbb{E}[S]/A \geq c$ may be rejected. For this purpose, it suffices to analyze null hypotheses of the form $\mathbb{E}[S] \leq \mu$ for all choices of μ .

As each X_i lies in the interval $[0, a_i]$, Hoeffding's inequality could be used to test such null hypotheses. However, we found that Hoeffding's inequality could be improved, yielding substantially smaller confidence intervals for the SDR in practice.

2.3 An improvement to Hoeffding's second inequality

We begin by introducing notation for the quantities that Hoeffding [1963] bounds. For any scalar $b \geq 0$, let \mathcal{M}_b denote the space of probability distributions with support on $[0, b]$.

For any module sizes $\mathbf{a} \in (\mathbb{R}^+)^m$ and fixed mean μ , let

$$\mathcal{M}_{\mathbf{a}, \mu} = \left\{ \mathbf{p} \in \prod_i \mathcal{M}_{a_i} : \sum_i E_{X_i \sim p_i}[X_i] \leq \mu \right\}.$$

We consider null hypotheses with the form

$$H_0 : \mathbf{X} \sim \left(\prod_i p_i \right), \mathbf{p} \in \mathcal{M}_{\mathbf{a}, \mu}.$$

Each null hypothesis of this form includes all cases in which $\mathbb{E}[S]$ is less than μ .

Given an observation $S = s$, we can test a null hypothesis using Chernoff-Cramér bounds. For any $\mathbf{p} \in \mathcal{M}_{\mathbf{a},\mu}$ and any threshold s , let

$$\varphi(\mathbf{p}, s) = \inf_{t \geq 0} \left(\sum_i \log E_{X_i \sim p_i}[\exp(tX_i)] - ts \right).$$

Upper bounds for $\mathbb{P}(S \geq s)$ are available in terms of φ from a Chernoff-Cramér bound:

$$\log \mathbb{P}_{\mathbf{X} \sim \prod_i p_i} \left(\sum_i X_i \geq s \right) \leq \varphi(\mathbf{p}, s).$$

With the observation $S = s$, we may thus reject H_0 whenever

$$\log \alpha \geq \max_{\mathbf{p} \in \mathcal{M}_{\mathbf{a},\mu}} \varphi(\mathbf{p}, s) \tag{2}$$

with type I error no greater than α . Henceforth, we denote the right-hand side of Equation (2) as $\varphi_{\mathbf{a},\mu}^*(s)$.

Hoeffding [1963] proposes bounds on $\varphi_{\mathbf{a},\mu}^*$. We review some of his findings. When $a_i = a_j$ for all i and j , Hoeffding gives an explicit formula for $\varphi_{\mathbf{a},\mu}^*$. When $a_i \neq a_j$ for some i and j , Hoeffding gives a bound on $\varphi_{\mathbf{a},\mu}^*$,

$$\varphi_{\mathbf{a},\mu}^* \leq -2(s - \mu)^2 / \sum a_i^2,$$

leading to the celebrated Hoeffding inequality. However, more powerful hypothesis tests can be performed by calculating $\varphi_{\mathbf{a},\mu}^*$ exactly. We now show a way this can be done.

We first apply Sion's minimax theorem (cf. [Komiya, 1988]) to show that $\varphi_{\mathbf{a},\mu}^*$ is the solution to a finite-dimensional minimax problem. The minimax theorem allows us to commute the inner one-dimensional minimization over $t \in \mathbb{R}^+$ with the outer infinite-dimensional maximization over $\mathbf{p} \in \mathcal{M}_{\mathbf{a},\mu}$. Once this has been done, the infinite-dimensional maximization problem can be reduced to a finite-dimensional form.

Theorem 2. *Let $\xi(a, t) = (\exp(at) - 1)/a$. Then,*

$$\varphi_{\mathbf{a},\mu}^*(s) = \min_{t \geq 0} \left(\max_{\substack{\tau \in \prod_i [0, a_i] \\ \sum_i \tau_i = \mu}} \sum_i \log(1 + \xi(a_i, t)\tau_i) - ts \right).$$

Next, we calculate how the finite-dimensional minimax problem in Theorem 2 can be solved using convex optimization.

Theorem 3. Let $\xi(a, t) = (\exp(at) - 1)/a$, $\text{clamp}(x, l, u) = \min(\max(x, l), u)$,

$$\tau_i^*(t, \lambda) = \text{clamp}\left(\frac{\xi(a_i, t) - \lambda}{\xi(a_i, t)\lambda}, 0, a_i\right),$$

and

$$g(t, \lambda) = \sum_i \log(1 + \xi(a_i, t)\tau_i^*(t, \lambda)) + \lambda\left(\mu - \sum_i \tau_i^*(t, \lambda)\right) - ts.$$

Then, g is convex and

$$\max_{\substack{\tau \in \prod_i [0, a_i] \\ \sum_i \tau_i = \mu}} \sum_i \log(1 + \xi(a_i, t)\tau_i) - ts = \min_{\lambda \geq 0} g(t, \lambda).$$

Moreover, the mapping $t \mapsto \min_{\lambda} g(t, \lambda)$ is convex and the mapping $\lambda \mapsto g(t, \lambda)$ is convex for each $t \geq 0$.

Theorem 3 suggests two methods by which the finite-dimensional minimax problem in Theorem 2 can be solved. One option is to directly minimize the two-dimensional convex function g . Another is to minimize the one-dimensional convex function $t \mapsto \min_{\lambda} g(t, \lambda)$, although each evaluation of this function requires solving a different one-dimensional convex optimization problem. In practice we found it slightly faster to minimize the two-dimensional convex function directly.

To assess the degree of improvement over Hoeffding's inequality, we simulated five random draws from the 100-dimensional simplex, each representing a vector \mathbf{a} of sizes for 100 modules. For each draw, we considered three different choices of mean, $\mu \in \{0.8, 0.9, 0.95\}$, and investigated the corresponding tail bounds $\varphi_{\mathbf{a}, \mu}^*$ given by Theorem 2. The three different values of μ correspond to sign disagreement rates of 20%, 10%, and 5%, respectively. For each choice, we used Hoeffding's inequality to upper bound $\mathbb{P}(S \geq s)$ under the assumption that $\mathbb{E}[S] = \mu$. We compare these upper bounds to the tightest Chernoff-Cramér

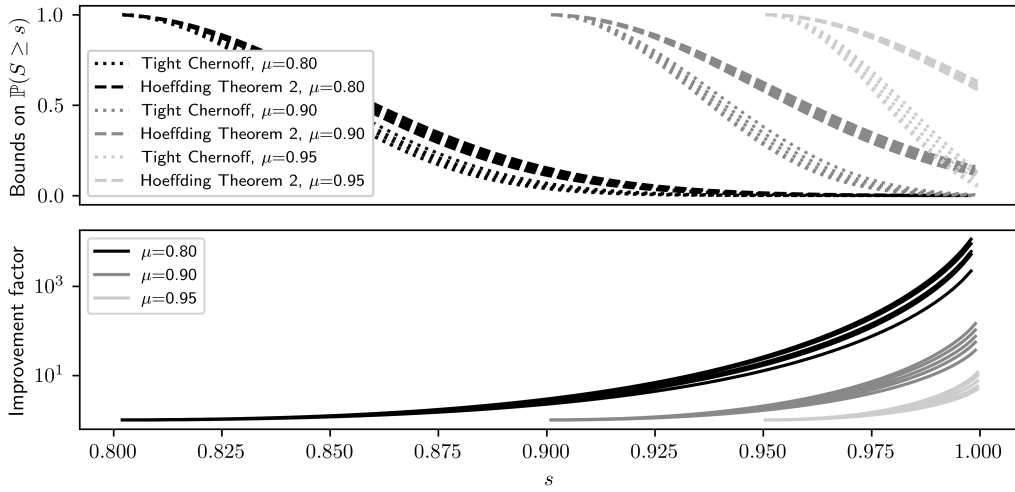


Figure 1: The tightest Chernoff-Cramér bounds are tighter than Hoeffding’s inequality. We consider three choices of fixed mean, $\mu \in \{.8, .9..95\}$. For each, we consider five randomly selected choices for the module sizes. We compare tail bounds based on Hoeffding’s inequality [Hoeffding, 1963, Theorem 2] with the tightest Chernoff-Cramér bounds; the latter are calculated using Theorem 2 and Theorem 3. The left plot shows the bounds. The right plot demonstrates the factor of improvement, showing ratios of the two bounds on a log scale.

bound under the same assumption. Figure 1 shows the results, indicating a wide range of cases in which the tighter bounds would lead to tighter confidence intervals on the SDR.

2.4 Error control

For many of the parameters investigated by a given breadth-first study, the results may be inconclusive as to the sign of the parameters. We then expect the overall sign error proportion in the estimates to be quite high.

If the overall sign error proportion is high, a sign error control method may be necessary to obtain insights from the study. That is, we need a method to use the data to select a subset of parameters \mathcal{S} and a sign estimate for each parameter such that the proportion of type S errors in the subset is typically small. By identifying a subset of estimates with few errors, we can still use the results of a study—even if the overall level of error among the proposed signs is high. Adopting nomenclature from false discovery rate literature, we refer to the parameters in this subset as discoveries. Discoveries for which the sign is incorrectly estimated are referred to as false discoveries.

Benjamini and Yekutieli [2005] suggest one sign error control method that requires modeling assumptions. In contrast, we propose a model-free sign error control method based on bounding the SDR.

The key idea is to estimate the SDR for various subsets of the parameters. Given a subset of parameter indices, $\mathcal{S} \subset \{1, \dots, n\}$, the SDP for a subset \mathcal{S} indicates the proportion of proposed signs for \mathcal{S} that have different signs from the validation signs for \mathcal{S} , and the SDR for the subset denotes the expected value of the SDP for the subset. We denote the corresponding values as $\text{SDP}_{\mathcal{S}}(\mathbf{Y}; \hat{\mathbf{y}})$ and $\text{SDR}_{\mathcal{S}}(\hat{\mathbf{y}})$. For example, applying Theorem 1, the type S error proportion in the proposed signs for \mathcal{S} is bounded by $\text{SDR}_{\mathcal{S}}(\hat{\mathbf{y}})/q$ if the

validation signs are q -faithful.

We propose the following approach to error control. Given a sequence of nested candidate subsets $\mathcal{S}_1 \subset \mathcal{S}_2 \subset \dots \subset \mathcal{S}_K$, we form an estimate U_k of $\text{SDR}_{\mathcal{S}_k}$ for each $k \in \{1, \dots, K\}$. For any target type S error proportion V^* , we let k^* denote the largest value such that $U_k \leq V^*/q$ and take our subset to be $\mathcal{S}^* = \mathcal{S}_{k^*}$. If the validation signs are q -faithful and $U_k \geq \text{SDR}_{\mathcal{S}_k}$ for each k , then the type S error proportion in \mathcal{S}^* is at most V^* .

This approach requires us to specify two ingredients: the candidate subsets and the SDR estimator. To aid us in specifying the candidate subsets, we assume that confidence scores are available for each proposed sign. For example, if a proposed sign \hat{y}_i is based on a previous study, it may have an associated p -value for the null hypothesis that $\theta_i = 0$. The negative logarithm of this p -value could be used as a confidence score. We denote the confidence score for parameter i as $\rho_i \in \mathbb{R}$. Our guarantees about the ability of our method to control error will not depend on how confidence scores are produced (for example, they could be based on misspecified models). Though error control is guaranteed for any confidence score, some ways of computing confidence may lead to more discoveries than others.

We consider three ways to specify the candidate subsets and the SDR estimator. Some lead to more discoveries, whereas others provide more extensive guarantees.

1. Using the SDP Assume, without loss of generality, that the parameters are ordered with respect to ρ such that $\rho_1 \geq \dots \geq \rho_n$. For each k , take $\mathcal{S}_k = \{1, \dots, k\}$. Take $U_k = \text{SDP}_{\mathcal{S}_k}$, which is an unbiased point estimate for $\text{SDR}_{\mathcal{S}_k}$.

2. Using non-simultaneous confidence intervals for the SDR Take the same candidate subsets used in the first way, but estimate the SDR as the upper bound of a

$(1-\alpha)$ confidence interval on $\text{SDR}_{\mathcal{S}_k}$. This approach incorporates our uncertainty. However, there are no formal guarantees about the subset \mathcal{S}^* selected in this way, as the confidence intervals are not considered simultaneously for all k .

3. Using simultaneous confidence for the SDR The third way controls error, with high probability. Instead of ordering parameters by confidence scores, order the modules by their average confidence scores:

$$i \geq j \implies \frac{1}{|P_i|} \sum_i \rho_i \leq \frac{1}{|P_j|} \sum_j \rho_j.$$

For each $k \in \{1, \dots, m\}$, take \mathcal{S}_k to be the union of $\{P_1, \dots, P_k\}$ and $\mathbf{U} \in [0, 1]^m$ to be the upper bounds of a simultaneous $(1-\alpha)$ confidence region for $(\text{SDR}_{\mathcal{S}_1}, \dots, \text{SDR}_{\mathcal{S}_m})$. Then, with probability $(1-\alpha)$, under the conditions of Theorem 1, the type S error proportion of the proposed signs among \mathcal{S}_k is less than U_k/q for all k . The following theorem shows how a submartingale inequality can be used to construct the needed confidence region.

Theorem 4. *Consider proposed signs $\hat{\mathbf{y}}$ and validation signs \mathbf{Y} organized into m modules P_1, \dots, P_m . Let $a_k = |P_k|$ denote the number of parameters in module k . Let \mathcal{S}_k denote the union of $\{P_1, \dots, P_k\}$. Let $\text{SDP}_{\mathcal{S}_k}$ denote the sign disagreement proportion between the proposed signs and validation signs in the subset k ; let $\text{SDR}_{\mathcal{S}_k}$ denote its expectation. Fix $\alpha \in [0, 1]$. Define $\hat{s}(\mu) = \max \{s : \varphi_{\mathbf{a}, \mu}^*(s) \leq \alpha\}$ and $\delta(s) = \max_{\mu: \varphi_{\mathbf{a}, \mu}^*(s) \geq \alpha} (\hat{s}(\mu) - \mu)$. Let*

$$U_k = \text{SDP}_{\mathcal{S}_k} + \frac{|\mathcal{S}_m|}{|\mathcal{S}_k|} (|\mathcal{S}_m| - \delta((1 - \text{SDP}_{\mathcal{S}_m}) |\mathcal{S}_m|) - \text{SDP}_{\mathcal{S}_m}).$$

Then, $\mathbb{P}(\text{SDR}_k \leq U_k \forall k) \geq 1 - \alpha$.

In Theorem 4, the upper bound U_m is identical to the bound that follows from computing a one-sided confidence interval for $\text{SDR}_{\mathcal{S}_m}$ by applying Theorem 2 directly. That is, the simultaneous confidence region for $(\text{SDR}_{\mathcal{S}_1}, \dots, \text{SDR}_{\mathcal{S}_m})$ gives the same bounds on

$\text{SDR}_{\mathcal{S}_m}$ as a single confidence interval on $\text{SDR}_{\mathcal{S}_m}$. This is a typical result when applying submartingale inequalities with Chernoff-Cramér bounds. On the other hand, the bounds U_k for $k < m$ are looser than those that would be obtained by constructing a confidence interval for $\text{SDR}_{\mathcal{S}_k}$ alone.

If \mathcal{S}^* is selected using the simultaneous confidence interval, what guarantees does it enjoy? To state the guarantee formally, we must define a new notion of error: the false sign discovery exceedance. This is a new variant of false discovery exceedance [Genovese and Wasserman, 2006].

Definition 5. Let \mathbf{Y} denote a vector of n sign estimates for a vector of parameters n $\boldsymbol{\theta}$. Let $S \subset \{1, 2, \dots, n\}$ denote a subset of the indices. The “false sign discovery exceedance” for target V^* is defined as

$$\mathbb{P}(|i \in S : Y_i \neq \text{sign}(\theta_i)| > V^*).$$

Assuming that the per-module agreement counts X_1, X_2, \dots, X_m are independent of each other, the validation signs and proposed signs are independent, and the validation signs are q -faithful, we have that the false sign discovery exceedance of \mathcal{S}^* is at most α .

We conclude our discussion of error control by noting that any method of estimating the SDR can be combined with arbitrary preprocessing of the parameter sets based on $\boldsymbol{\rho}$. We give three representative examples. First, for each module, we could ignore all but the ten parameters with the largest confidence scores. Second, we could order the modules in descending order by average confidence score and discard the latter half of the modules. Third, we could ignore all parameters i for which ρ_i failed to exceed a predetermined threshold. For any of these preprocessing examples, we could apply the preprocessing and then apply any of the error control options described above. In general, because $\boldsymbol{\rho}$ is conditioned upon in the probability calculations and assumed independent of the validation

signs, any such preprocessing would not interfere with the type S error guarantees.

3 Simulations and case studies

To probe the advantages and limitations of our model-free methods for error assessment and control, we conducted a series of simulations and case studies. The first investigation showed that our method for error control avoids the pitfalls of two model-based methods, one based on the work of Benjamini and Yekutieli [2005] and the other based on the work of Li et al. [2011]. We then used the SDR to assess the error of a new protocol for preprocessing cell-perturbation measurements (Section 3.2). Error assessment based on the SDR showed that the new preprocessing protocol led to better error bounds. Finally, we examined a case where an SDR-based error control method made more discoveries than a model-based error control method (Section 3.3).

3.1 Error control simulations

In this section, we consider three sign error control methods. To better understand the different methods, we simulated data in which the parameter values were known. First, we drew $n = 50,000$ parameters, $\theta_1 \dots \theta_n$, from a standard normal distribution, $\mathcal{N}(0, 1)$. We then simulated two replicates of a study for estimating the parameters. We assumed each replicate's estimate for each θ_i was distributed according to $\mathcal{N}(\theta_i, \tau_i^2)$. We constructed the variances τ_i^2 in terms of two coefficients: σ and k . For 90% of the parameters we took the variance to be σ^2 ; for 10% of the parameters we took it to be $k\sigma^2$. This represents the reality that a study may be well-suited for estimating some parameters but less well-suited for estimating others. We varied σ between 0.1 and 1.0 and varied k between 1 and 10.

We compared three sign error control methods on this dataset: an approach based on

SDR, an approach based on the false sign discovery rate method proposed by Benjamini and Yekutieli [2005], and an approach based on the Irreproducible Discovery Rate (IDR) [Li et al., 2011].

The first method uses an approach from Section 2.4: construct nested subsets of the parameters and select the largest subset for which the observed SDP does not exceed 5%. This method is designed to control the type S error proportion at a 10% level.

The second method combines a simple parametric model with the method of Benjamini and Yekutieli [2005] for controlling false sign discovery rates. Consider a model specifying that the estimate for θ_i is distributed according to $\mathcal{N}(\theta_i, \tilde{\tau}^2)$. This model has been considered by Zhao et al. [2020] for similar data and in many respects matches the true data-generating process of our simulation. However, this model assumes that the variance of every estimate is the same. This model misspecification leads to incorrect inferences. Remedying this misspecification would be difficult: it would be challenging to estimate the variance for all n parameters because there are only two independent observations for each. Assuming $\tau_i^2 = \tilde{\tau}^2$ for each i makes it straightforward to estimate each τ_i^2 , at the cost of potentially serious model misspecification. Once $\tilde{\tau}$ has been estimated, we can apply the method of Benjamini and Yekutieli [2005] to control the false sign discovery rate at the 10% level. The method of Benjamini and Yekutieli [2005] is valid under the following assumptions: the estimate for θ_i must grow stochastically with θ_i and the distribution of the estimate under the null hypothesis that $\theta_i = 0$ must be known. We applied the method under the false premise that all estimates are normally distributed with common variance $\tilde{\sigma}^2$, and investigated how this misspecification affects our conclusions.

The third method we consider uses the Irreproducible Discovery Rate (IDR) [Li et al., 2011]. This method requires the user to specify a scalar confidence score for each parameter-

replicate pair. It then produces a coefficient for each parameter. After applying the method, practitioners are encouraged to focus on parameters with smaller coefficient values. This method produces these coefficients by assuming that the copula of confidence scores from different replicates can be modeled as a two-component Gaussian mixture model. The parameters of the mixture model are fit to the data. For each parameter, the coefficient is computed as the posterior probability that the parameter arose from the mixing component corresponding to lower confidence scores. This coefficient is termed the local irreproducible discovery rate. This method was not originally designed for handling signed parameter estimation, so to apply it in our setting, we treat the positive cases and negative cases separately. Parameters for which the two replicates yield opposite signs are assigned an irreproducibility score of $1/2$. We apply the IDR to our error control problem by selecting all parameters where the local irreproducibility discovery rate is below 10%. This method relies on a model that is misspecified for our simulation and presumably many real-world datasets; it assumes the copula takes the form of a two-component mixture model and that “important” parameters arise only from one of those mixing components.

Figure 2 compares these three methods. All made many true discoveries when the noise level σ^2 was not too high. All methods also controlled error at the target level when $k = 1$; in this case, at least the second method’s model was specified correctly. However, when k and σ^2 were large, the second method had sign error proportions as high as 43% and the third method had sign error proportions as high as 36%. These methods failed to control type S error proportions at their target levels. The SDR-based approach always controlled type S error, keeping it below its target level.

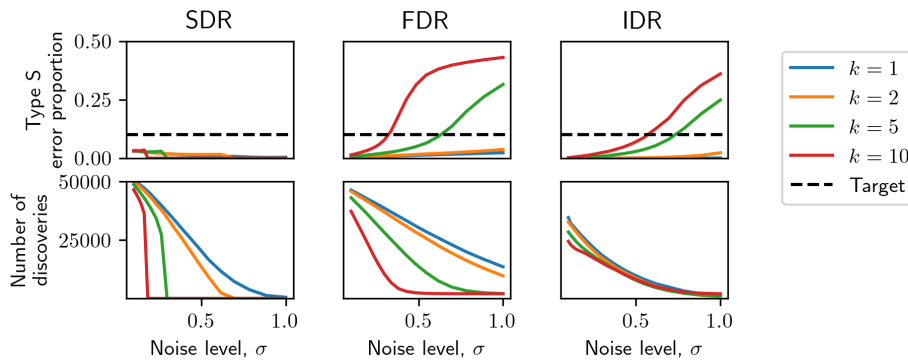


Figure 2: Comparing the SDR approach with alternatives for error control in simulated data. When k and σ^2 are large, it is challenging to accurately estimate the signs of the parameters. In this regime, the SDR-based method made no discoveries. Other methods made some discoveries, but a high proportion of these were false discoveries.

3.2 Error assessment in L1000 data

L1000 is a protocol developed by Subramanian et al. [2017b] for perturbing cells with small molecules and measuring the change in gene expression. The protocol involves collecting real-valued fluorescence measurements for each collection of cells. The protocol defines an algorithm for estimating gene expression from these values. Qiu et al. [2020] developed a new algorithm for reanalyzing the same fluorescence measurements. We refer to the original method as L1000A and the new method as L1000B. We sought to assess which method yields more accurate results.

Both protocols specify more than a series of steps in a laboratory: they also specify a model for how the estimates generated by the study should be interpreted, indicating a noise level for each estimate. For each parameter of interest, both methods produce an estimate. In both protocols, measurement noise is presumed to be Gaussian, and the scale of each parameter is normalized by an estimate of the measurement error such that the

measurement variance is exactly one. The sign of θ_i can be estimated by the sign of $\hat{\theta}_i$; this estimate has a lower chance of being wrong when the magnitude of θ_i is large. We used the protocols’ error models, together with the directional false discovery rate control method of Benjamini and Yekutieli [2005], to select a subset of parameters.

If the error models posited by the protocols are correct, the L1000A method appears superior. When analyzing a single replicate with a false sign discovery error rate target of 10%, the method of Benjamini and Yekutieli [2005] made 138,009 discoveries for L1000A and 0 discoveries for L1000B. This suggests that the original L1000A method is more useful for discovering parameters. However, our use of Benjamini-Hochberg method to identify these discoveries was only valid if the models posited by the protocols are correct.

To justify the superiority of L1000B, the authors [Qiu et al., 2020] noted that L1000B yielded more consistent answers across replicates than L1000A did. The authors further argued that the measurement noise may have been incorrectly assessed for the L1000A estimates. However, these authors did not have a rigorous way to connect their observation about estimator replicability to a notion of estimator error. Theorem 1 provides the necessary link. Qiu et al. [2020] also had no way to show that the differences in consistency were above a level to be expected from chance. Theorem 2 allows us to see that the differences were indeed statistically significant.

We began by computing the SDP for both L1000A and L1000B, assuming faithful validation signs. The data contains three replicates; we used two replicates to generate our proposed signs and the final replicate for the validation signs. See Appendix A for additional details on how these values were constructed. To compute the SDP, we computed the proportion of disagreements between the proposed signs and validation signs. Figure 3 demonstrates the process of making this calculation on L1000B data for a representative

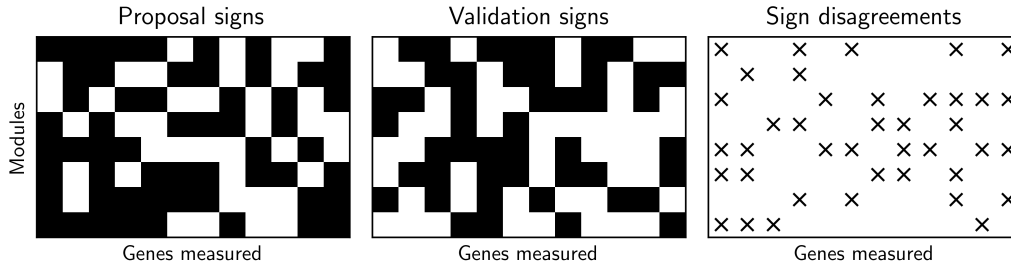


Figure 3: The SDP in L1000B data. The SDP is computed by taking the proportion of parameters where the proposed signs and validation signs disagree. Each plot above represents a matrix in which rows correspond to modules and columns correspond to genes measured; each cell in the grid corresponds to a question we sought to answer: does the stimulus investigated by a particular module upregulate or downregulate a particular gene? The left plot indicates answers to these questions given by the proposed signs, with white indicating upregulation and black indicating downregulation. The middle plot indicates answers given by the validation signs. The right plot indicates cases in which the two answers disagree.

subset of the parameters of interest; the figure shows the proposed signs, validation signs, and disagreements for these parameters. Visual inspection shows that the data is noisy; the different replicates disagree in many instances.

The SDP in L1000A is 40% and the SDP in L1000B is 38%. These values are above 25%, so the bounds of Theorem 1 yield trivial results for both protocols under a faithfulness assumption; we obtain type S error proportion bounds in excess of 50%. These high SDP values are consistent with a recent article suggesting that the average accuracy of the estimates in L1000A data may be lower than had been supposed [Lim and Pavlidis, 2021].

The SDP does not show evidence of high overall accuracy in either protocol, but that does not imply that the results of these protocols cannot be used to produce accurate

estimates for a subset of the parameters. Toward this end, we investigated sign error proportions for various subsets of parameters.

For each protocol, we obtained a confidence score ρ_i for each parameter θ_i by taking the absolute value of the estimate $\hat{\theta}_i$. Crucially, this confidence score does not depend on the validation signs. As discussed in Section 2.4, we were therefore free to use $\boldsymbol{\rho} = \{\rho_1, \dots, \rho_n\}$ to define subsets of parameters and to estimate the SDR for each subset; Theorem 1 remains valid for each subset. For this case study, we considered subsets of the form $\mathcal{S}_t = \{i : \rho_i \geq t\}$. For each t , for each protocol, we computed $\text{SDP}_{\mathcal{S}_t}$ along with a 95% two-sided confidence interval for $\text{SDP}_{\mathcal{S}_t}$. The confidence intervals were produced using Theorem 2. Each stimulus corresponds to one module; that is, we assumed that the disagreements between $\hat{\mathbf{y}}$ and \mathbf{Y} for parameters regarding each stimulus were independent of the disagreements concerning other stimuli.

Sweeping over a variety of thresholds t , Figure 4 plots the number of parameters in each subset, $|\mathcal{S}_t|$, against the corresponding values of $\text{SDP}_{\mathcal{S}_t}$. For example, in L1000B we found a subset of 100,000 parameters with SDP of 5%, suggesting a type S error proportion below 10%. On the other hand, nontrivial error bounds cannot be identified for L1000A on any subset of data. Moreover, the largest SDPs in the L1000A data appear among subsets of parameters with the largest confidence scores; such subsets are shown toward the left side of Figure 4. We might expect estimators with high confidence scores to commit fewer errors, so this result is somewhat surprising. This evidence supports the conjecture from Qiu et al. [2020] that a small proportion of the fluorescence measurements include profound anomalies, and that the original heuristic algorithm overestimates effect sizes and underestimates error levels in these anomalous readings.

Figure 4 also indicates 95% confidence intervals for $\text{SDR}_{\mathcal{S}_t}$ for each t , computed using

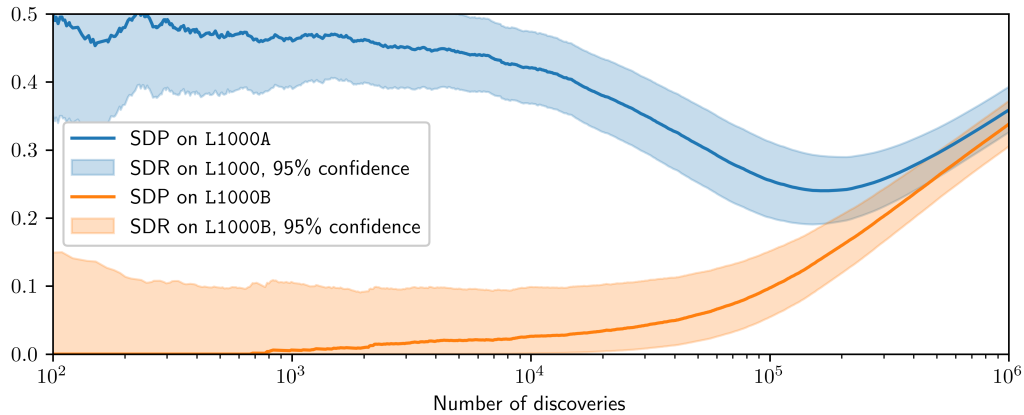


Figure 4: The SDR suggests lower type S error proportions in the estimates of a new protocol. For each threshold t , for both the L1000A and L1000B protocols, we estimated the SDR on the subset of parameters whose confidence scores are greater than t . We then plot the subset sizes against the corresponding SDR estimates, sweeping over all thresholds. To estimate the SDR, we took the SDP as a point estimate and used Theorem 2 to produce a 95% two-sided confidence interval. At each fixed number of parameters, we found that L1000B yields lower SDR estimates.

Theorem 2. Such intervals could also have been computed using Hoeffding’s inequality, but the resulting confidence intervals are broader than necessary, typically by a factor of roughly 1.5. For example, considering the subset of parameters \mathcal{S}_t with 5000 parameters in total, the SDP is 2.0%, Theorem 2 yielded an upper bound of 9.6% for the $\text{SDR}_{\mathcal{S}_t}$, whereas the Hoeffding inequality yielded an upper bound of 14.2%.

3.3 Error control in L1000B data

In the preceding section, we assessed that the proportion of type S errors in certain subsets of the L1000B estimates is less than 1%. We now consider our uncertainty about this assessment more carefully, following the methods outlined in Section 2.4.

As in the previous section, we constructed a nested sequence of subsets, with each subset defined by selecting parameters whose confidence scores exceed a threshold. We sought to identify the subsets in this sequence for which the SDR was below a threshold. We considered three approaches to estimate the SDR in each of these subsets. The first approach uses the SDP for each subset, which is an unbiased estimate. The second uses a non-simultaneous one-sided 98.75% confidence interval for each subset. The third applies Theorem 4 four times, yielding four 98.75% simultaneous confidence regions; these are merged to yield a single 95% simultaneous confidence region (cf. Appendix D for more details). In all cases, we assumed that each module includes only one parameter, i.e., the disagreements between the proposed signs and the validation signs are all independent indicator variables.

Figure 5 shows how different estimators of the SDR led to different numbers of discoveries. For example, suppose that we were to target a type S error proportion of 10% and assume the validation signs are faithful. Taking the SDPs as our estimates we found 40,416

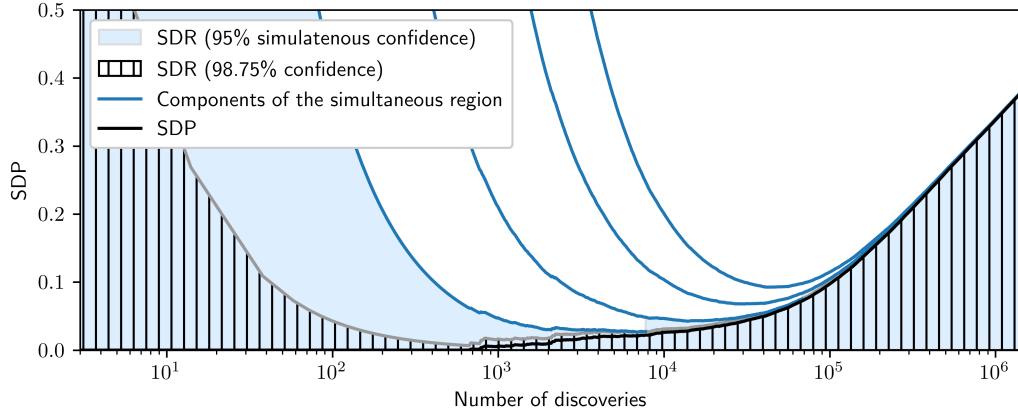


Figure 5: Simultaneous confidence intervals for the SDR in different subsets of parameters. For each threshold t , we estimated the SDR on the subset of parameters whose confidence scores are greater than t . We then plotted the subset sizes against the corresponding SDR estimates, sweeping over all thresholds. In estimating the SDRs, we considered three possibilities: the SDPs, 98.75% one-sided (non-simultaneous) confidence intervals, and a single 95% confidence region which is simultaneous over all thresholds considered. The last is formed by merging four simultaneous 98.75% confidence regions.

discoveries with SDP less than 5% (and thus a type S error proportion less than 10%, per Theorem 1). Using the upper bounds of the 98.75% one-sided confidence intervals for the SDRs leads to a more conservative conclusion; we made 35,502 discoveries. Finally, using the simultaneous confidence region, we made 31,284 discoveries.

How do these SDR-based approaches to error control compare with model-based methods? We applied the Benjamini-Hochberg method to a combination of all three replicates of the L1000B data. Under the protocol’s model, the estimators from each replicate are independent, unbiased, and normally distributed with unit variance. Therefore, we summed the estimators over the replicates, divided by $\sqrt{3}$, computed two-sided p -values, and applied the method of Benjamini and Yekutieli [2005] to identify a subset of parameters in which the expected type S error proportion was controlled. This approach discovered only 24,629 parameters. Figure 6 in Appendix C demonstrates the manner in which this subset of parameters was calculated, plotting the model-based p -values against the Benjamini-Hochberg thresholds on a log-log scale. The Benjamini-Hochberg approach made fewer discoveries than even the most conservative SDR-based approach. This could be due to inherently conservative behavior in the Benjamini-Hochberg procedure, but we conjecture that it is largely due to overestimated measurement noise levels in the L1000B data.

4 Connections to existing work in error control

Our method for error control has connections to many other methods in the literature. For example, as we investigated in our simulations and case studies, the Benjamini-Hochberg multiple testing procedure [Benjamini and Yekutieli, 2005] can be also used to select subsets of parameters while controlling the expected number of sign errors committed among the subset. Our method differs from existing methods through its model-free design: it allows

error assessment and error control without assuming the data follow a known parametric probability distribution. For example, many methods including Benjamini-Hochberg require users to provide p -values that must be superuniform under certain null hypotheses. These may be difficult to provide, as even p -values from nonparametric tests such as the Mann-Whitney U test require many independent observations within a single module. In practice, it may be impossible to obtain multiple independent observations of the same parameter due to unobserved variables affecting the entire module (e.g., the humidity level in the room [Stein et al., 2015]). By contrast, the SDR requires only that the modules are independent of each other and faithful.

The model-free nature of our approach bears some similarity to knockoff methods [Barber and Candès, 2015]. In brief, knockoff methods select a subset of regressors that are important in predicting a response. As long the joint distribution of the regressors is well understood, knockoffs make it possible to test hypotheses about the relationship between the responses and the regressors without assuming any parametric model for the conditional distribution of the response given the regressors. Knockoffs have proven their value in a variety of settings, including cases that focus on controlling type S errors [Cao et al., 2023]. However, the SDR applies to a different problem. It helps identify a set of estimators with low type S error proportion, without requiring the user to single out one variable as the “response” variable. It is also a fully model-free method. Knockoffs require no model for the conditional distribution of the response but do require a model of the joint distribution of the regressors.

Finally, our approach to error control requires confidence scores that can be used to order parameters, and this resembles some existing error control methods that use auxiliary information to improve power in multiple testing scenarios (e.g., Lei and Fithian [2018]).

The SDR approach differs in that it requires three objects: one set of sign estimates, confidence scores for each of these estimates, and another set of sign estimates from an independent study. By contrast, existing error control approaches using auxiliary information require a different set of objects, namely auxiliary information about the parameters and a superuniform p -value for each parameter.

5 Conclusions

Accurate type S error assessment is useful for many reasons. It enables practitioners to control type S error, allowing them to identify which results are worthy of future investigation. It enables practitioners to compare the error of different protocols to determine their relative merits. Finally, it enables practitioners to recognize that error rates may be larger than supposed. For example, although the original L1000 data was published in 2017, it took four years for concerns about its replicability to rise to the level of a publication [Lim and Pavlidis, 2021]. If the original experimentalists had calculated the SDP, some of these problems could have been identified immediately. Developing and implementing protocol-specific strategies to evaluate error is difficult. Simple best practices for assessing error that can be applied across experimental modalities would alleviate this burden.

Software. Our Python software for computing tail bounds using Theorem 3 can be found at <https://github.com/prob-ml/tighter-hoeffding>.

Acknowledgements. We thank Robert Barton, Meena Subramaniam, Maxime Dhainaut, and Drausin Wulsin for introducing us the scientific problems that motivated this research.

Funding. This research was funded by Immunai Inc.

Supplementary material. Appendices (including an appendix for all proofs) can be

found in the supplementary material document associated with this submission.

References

- Rina Foygel Barber and Emmanuel J. Candès. Controlling the false discovery rate via knockoffs. *The Annals of Statistics*, 43(5):2055 – 2085, 2015.
- Yoav Benjamini and Daniel Yekutieli. False Discovery Rate–Adjusted Multiple Confidence Intervals for Selected Parameters. *Journal of the American Statistical Association*, 100(469):71–81, March 2005.
- Yang Cao, Xinwei Sun, and Yuan Yao. Split knockoffs for multiple comparisons: Controlling the directional false discovery rate. *Journal of the American Statistical Association*, (just-accepted):1–21, 2023.
- Mengjie Chen, Zhao Ren, Hongyu Zhao, and Harrison Zhou. Asymptotically normal and efficient estimation of covariate-adjusted gaussian graphical model. *Journal of the American Statistical Association*, 111(513):394–406, 2016.
- Siamak Zamani Dadaneh, Paul de Figueiredo, Sing-Hoi Sze, Mingyuan Zhou, and Xiaoning Qian. Bayesian gamma-negative binomial modeling of single-cell rna sequencing data. *BMC genomics*, 21:1–10, 2020.
- E.H. Davidson. *Genomic Regulatory Systems: In Development and Evolution*. Elsevier Science, 2001.
- Andrew Gelman and Francis Tuerlinckx. Type S error rates for classical and Bayesian single and multiple comparison procedures. *Computational Statistics*, 15(3):373–390, 2000.

- Christopher R Genovese and Larry Wasserman. Exceedance control of the false discovery proportion. *Journal of the American Statistical Association*, 101(476):1408–1417, 2006.
- Wassily Hoeffding. Probability Inequalities for Sums of Bounded Random Variables. *Journal of the American Statistical Association*, 58(301):13–30, 1963.
- Hidetoshi Komiya. Elementary proof for sion’s minimax theorem. *Kodai mathematical journal*, 11(1):5–7, 1988.
- Lihua Lei and William Fithian. AdaPT: an interactive procedure for multiple testing with side information. *Journal of the Royal Statistical Society Series B: Statistical Methodology*, 80(4):649–679, 2018.
- Qunhua Li, James B Brown, Haiyan Huang, and Peter J Bickel. Measuring reproducibility of high-throughput experiments. *The Annals of Applied Statistics*, 5(3):1752–1779, 2011.
- Nathaniel Lim and Paul Pavlidis. Evaluation of connectivity map shows limited reproducibility in drug repositioning. *Scientific Reports*, 11(1):1–14, 2021.
- Maya B Mathur and Tyler J VanderWeele. New statistical metrics for multisite replication projects. *Journal of the Royal Statistical Society Series A: Statistics in Society*, 183(3): 1145–1166, 2020.
- Yue Qiu, Tianhuan Lu, Hansaim Lim, and Lei Xie. A Bayesian approach to accurate and robust signature detection on LINCS L1000 data. *Bioinformatics*, 36(9):2787–2795, 2020.
- Paul R Rosenbaum. Conditional permutation tests and the propensity score in observational studies. *Journal of the American Statistical Association*, 79(387):565–574, 1984.

Ralf Schmidt, Zachary Steinhart, Madeline Layeghi, Jacob W Freimer, Raymund Bueno, Vinh Q Nguyen, Franziska Blaeschke, Chun Jimmie Ye, and Alexander Marson. CRISPR activation and interference screens decode stimulation responses in primary human T cells. *Science*, 375(6580), 2022.

Bowen Shi, Yanyuan Wu, Haojie Chen, Jie Ding, and Jun Qi. Understanding of mouse and human bladder at single-cell resolution: integrated analysis of trajectory and cell-cell interactive networks based on multiple scRNA-seq datasets. *Cell Proliferation*, 55(1): e13170, 2022.

Eric Shifrut, Julia Carnevale, Victoria Tobin, Theodore L Roth, Jonathan M Woo, Christina T Bui, P Jonathan Li, Morgan E Diolaiti, Alan Ashworth, and Alexander Marson. Genome-wide CRISPR screens in primary human T cells reveal key regulators of immune function. *Cell*, 175(7):1958–1971, 2018.

Sanjay R Srivatsan, José L McFaline-Figueroa, Vijay Ramani, Lauren Saunders, Junyue Cao, Jonathan Packer, Hannah A Pliner, Dana L Jackson, Riza M Daza, Lena Christiansen, et al. Massively multiplex chemical transcriptomics at single-cell resolution. *Science*, 367(6473):45–51, 2020.

Caleb K Stein, Pingping Qu, Joshua Epstein, Amy Buros, Adam Rosenthal, John Crowley, Gareth Morgan, and Bart Barlogie. Removing batch effects from purified plasma cell gene expression microarrays with modified combat. *BMC Bioinformatics*, 16(1):1–9, 2015.

Aravind Subramanian, Rajiv Narayan, Steven M Corsello, David D Peck, Ted E Natoli, Xiaodong Lu, Joshua Gould, John F Davis, Andrew A Tubelli, Jacob K Asiedu, et al. A

next generation connectivity map: L1000 platform and the first 1,000,000 profiles. *Gene Expression Omnibus*, 2017a. Accession GSE70138.

Aravind Subramanian, Rajiv Narayan, Steven M Corsello, David D Peck, Ted E Natoli, Xiaodong Lu, Joshua Gould, John F Davis, Andrew A Tubelli, Jacob K Asiedu, et al. A next generation connectivity map: L1000 platform and the first 1,000,000 profiles. *Cell*, 171(6):1437–1452, 2017b.

Lina Wang, Yongjun Piao, Dongyue Zhang, Wenli Feng, Chenchen Wang, Xiaoxi Cui, Qian Ren, Xiaofan Zhu, and Guoguang Zheng. FBXW11 impairs the repopulation capacity of hematopoietic stem/progenitor cells. *Stem Cell Research & Therapy*, 13(1):1–14, 2022.

Qiuyu Wu and Xiangyu Luo. Estimating heterogeneous gene regulatory networks from zero-inflated single-cell expression data. *The Annals of Applied Statistics*, 16(4):2183 – 2200, 2022.

Shishuai Xie, Wanxiang Niu, Feng Xu, Yuping Wang, Shanshan Hu, and Chaoshi Niu. Differential expression and significance of miRNAs in plasma extracellular vesicles of patients with Parkinson’s disease. *International Journal of Neuroscience*, 132(7):673–688, 2022.

Sojung Yoon, Sung Eun Kim, Younhee Ko, Gwang Hun Jeong, Keum Hwa Lee, Jinhee Lee, Marco Solmi, Louis Jacob, Lee Smith, Andrew Stickley, et al. Differential expression of microRNAs in Alzheimer’s disease: A systematic review and meta-analysis. *Molecular Psychiatry*, 27(5):2405–2413, 2022.

Yi Zhao, Matthew G Sampson, and Xiaoquan Wen. Quantify and control reproducibility in high-throughput experiments. *Nature Methods*, 17(12):1207–1213, 2020.

Supplementary Material for “Model-Free Error Assessment for Breadth-First Studies, with Applications to Cell-Perturbation Experiments”

A Dataset acquisition and pre-processing

In this work we use two datasets, which we refer to as L1000A and L1000B.

The L1000A dataset was originally presented by Subramanian et al. [2017b] and deposited to the GEO database [Subramanian et al., 2017a]. It can be viewed at several levels of pre-processing; we elected to view after it had been preprocessed to what is referred to as level 4. The data in this level comprises a z -score for each replicate for each perturbation for each dosage for each cell type for each gene. The data can be downloaded from GEO accession GSE70138 (cf. <https://www.ncbi.nlm.nih.gov/geo/query/acc.cgi>).

This dataset was reanalyzed by Qiu et al. [2020], leading to an alternative dataset, also containing z -scores. This data is available from the following URL:

<https://github.com/njpipeorgan/L1000-bayesian>.

Both datasets include information about 978 genes for many different perturbations applied to many different cell-types at many different dosages. In this work we focus on the parameters concerning A375 cells when subjected to the highest dosages considered for each perturbation.

B Proofs

Theorem. *If $\mathbf{Y} \in \{-1, 1\}^n$ are faithful validation signs for $\boldsymbol{\theta}$, then the type S error proportion is bounded by $V(\hat{\mathbf{y}}, \boldsymbol{\theta}) \leq \text{SDR}(\hat{\mathbf{y}})/q$.*

Proof. Observe that

$$\begin{aligned}
 \text{SDR} &= \frac{1}{n} \left(\sum_{i: \hat{y}_i = \text{sign}(\theta_i)} \mathbb{P}(Y_i \neq \hat{y}_i) + \sum_{i: \hat{y}_i \neq \text{sign}(\theta_i)} \mathbb{P}(Y_i \neq \hat{y}_i) \right) \\
 &= \frac{1}{n} \left(\sum_{i: \hat{y}_i = \text{sign}(\theta_i)} \mathbb{P}(Y_i \neq \text{sign}(\theta_i)) + \sum_{i: \hat{y}_i \neq \text{sign}(\theta_i)} \mathbb{P}(Y_i = \text{sign}(\theta_i)) \right) \\
 &\geq \frac{1}{n} \left(0 + \sum_{i: \hat{y}_i \neq \text{sign}(\theta_i)} q \right) \\
 &= V(\hat{\mathbf{y}}, \boldsymbol{\theta})q.
 \end{aligned}$$

□

To prove the next result, Theorem 2 in the main body of this paper, we view $\mathcal{M}_{\mathbf{a}, \mu}$ as a topological vector space. For any scalar $b \geq 0$, let \mathcal{M}_b denote the space of probability measures with support on $[0, b]$. Endowing \mathcal{M}_b with the weak-* topology, we view \mathcal{M}_b as a topological vector space. Note that \mathcal{M}_b is compact and convex. For any subexperiment sizes $\mathbf{a} \in (\mathbb{R}^+)^m$ and fixed mean μ , let

$$\mathcal{M}_{\mathbf{a}, \mu} = \left\{ \mathbf{p} \in \prod_i \mathcal{M}_{a_i} : \sum_i \mathbb{E}_{X_i \sim p_i}[X_i] \leq \mu \right\}.$$

Here

$$\prod_i \mathcal{M}_{a_i}$$

denotes a direct sum of a topological vector spaces. For example, if $\mathbf{p} \in \mathcal{M}_{\mathbf{a}, \mu}$ then $\mathbf{p} = (p_1, \dots, p_m)$ where each $p_i \in \mathcal{M}_{a_i}$. Recall that addition is computed in the following manner for such direct sum spaces: for any $\mathbf{p}, \mathbf{q} \in \mathcal{M}_{\mathbf{a}, \mu}$, $(\mathbf{p} + \mathbf{q}) = ((p_1 + q_1), \dots, (p_m + q_m))$. This seemingly excessive formality is necessary to clarify that $\mathcal{M}_{\mathbf{a}, \mu}$ is, in fact, convex.

Theorem. Let $\xi(a, t) = (\exp(at) - 1)/a$. Then,

$$\varphi_{\mathbf{a}, \mu}^*(s) = \min_{t \geq 0} \left(\max_{\substack{\tau \in \prod_i [0, a_i] \\ \sum_i \tau_i = \mu}} \sum_i \log(1 + \xi(a_i, t)\tau_i) - ts \right).$$

Proof. Fix s . Let

$$f(t, \mathbf{p}) = \sum_i \log \mathbb{E}_{X_i \sim p_i} [\exp(tX_i)] - ts.$$

Our object of interest is may be given as $\min_t \max_{\mathbf{p}} f(t, \mathbf{p})$. Our first step is to reverse the order of the minimization and maximization by applying Sion's minimax theorem [Komiya, 1988]. We observe the following.

- f is convex with respect to t , as it is the sum of cumulant generating functions.
- f is concave with respect to \mathbf{p} , due to Jensen's inequality.
- f is continuous with respect both \mathbf{p} and t .
- $\mathcal{M}_{\mathbf{a}, \mu}$ is both convex and compact.
- $[0, \infty)$ is convex (though not compact).

Sion's minimax theorem thus shows that

$$\min_{t \geq 0} \max_{\mathbf{p} \in \mathcal{M}_{\mathbf{a}, \mu}} f(t, \mathbf{p}) = \min_{t \geq 0} \max_{\mathbf{p} \in \mathcal{M}_{\mathbf{a}, \mu}} f(t, \mathbf{p}).$$

For any fixed t , the maximization of f may be reduced to a finite-dimensional problem.

First, we rewrite the maximization problem by introducing auxiliary variables, as follows:

$$\begin{aligned}
\max_{\mathbf{p}, \tau} \quad & f(t, \mathbf{p}) \\
\text{s.t.} \quad & \tau_i \in [0, a_i] \\
& p_i \in \mathcal{M}_{a_i} \\
& \tau_i = \sum_i \mathbb{E}_{X_i \sim p_i} [X_i] \\
& \sum_i \tau_i \leq \mu
\end{aligned}$$

For any fixed τ , Hoeffding [Hoeffding, 1963, proof of Theorem 1] showed that the cumulant generating functions can be maximized by setting each p_i to be a scaled Bernoulli random variable, namely

$$p_i = \delta_0 \left(1 - \frac{\tau_i}{a_i}\right) + \delta_{a_i} \frac{\tau_i}{a_i}$$

where δ_x represents the point mass at x . Under this distribution,

$$\log \mathbb{E}_{p_i} [\exp(tX_i)] = \log(1 + \xi(a_i, t)\tau_i).$$

Note that this is monotone increasing in τ , so the constraint $\sum_i \tau_i \leq \mu$ may be replaced with the constraint $\sum_i \tau_i = \mu$ without changing the result. Our problem thus reduces to the desired form.

□

Theorem. Let $\xi(a, t) = (\exp(at) - 1)/a$, $\text{clamp}(x, l, u) = \min(\max(x, l), u)$,

$$\tau_i^*(t, \lambda) = \text{clamp}\left(\frac{\xi(a_i, t) - \lambda}{\xi(a_i, t)\lambda}, 0, a_i\right),$$

and

$$g(t, \lambda) = \sum_i \log(1 + \xi(a_i, t)\tau_i^*(t, \lambda)) + \lambda \left(\mu - \sum_i \tau_i^*(t, \lambda)\right) - ts.$$

Then, g is convex and

$$\max_{\substack{\tau \in \prod_i [0, a_i] \\ \sum_i \tau_i = \mu}} \sum_i \log(1 + \xi(a_i, t)\tau_i) - ts = \min_{\lambda \geq 0} g(t, \lambda).$$

Moreover, the mapping $t \mapsto \min_{\lambda} g(t, \lambda)$ is convex and the mapping $\lambda \mapsto g(t, \lambda)$ is convex for each $t \geq 0$.

Proof. For any fixed $t \geq 0$, we begin by rewriting the maximization problem in terms of

$$f(\tau; t) = \begin{cases} \sum_i \log(1 + \xi(a_i, t)\tau_i) - ts & \text{if } \tau \in \prod_i [0, a_i] \\ -\infty & \text{else.} \end{cases}$$

That is, we incorporate the inequality constraints into the domain of optimization. The maximization problem of interest is equivalent to

$$\max_{\tau: \sum_i \tau_i = \mu} f(\tau; t).$$

The associated Lagrangian function is given by

$$\mathcal{L}(\tau, \lambda; t) = \sum_i \log(1 + \xi(a_i, t)\tau_i) + \lambda \left(\mu - \sum_i \tau_i \right) - ts.$$

For any fixed $t \geq 0$, observe that $\xi(a_i, t)$ is positive and thus $\tau \mapsto \mathcal{L}(\tau, \lambda; t)$ is concave. The argument maximizing $\tau \mapsto \mathcal{L}(\tau, \lambda; t)$ is given by $\tau_i^*(t, \lambda)$. Thus $g(t, \lambda) = \max_{\tau} \mathcal{L}(\tau, \lambda; t)$, the Lagrangian dual for a convex optimization problem with convex constraints. There is at least one feasible point, namely $\tau_i = a_i \mu / \sum_j a_j$, so strong duality holds and

$$\max_{\substack{\tau \in \prod_i [0, a_i] \\ \sum_i \tau_i = \mu}} \sum_i \log(1 + \xi(a_i, t)\tau_i) - ts = \min_{\lambda} g(t, \lambda)$$

as desired.

We now demonstrate that g is convex. First, observe that \mathcal{L} is affine in λ and convex in t . Thus g is a pointwise maximum of a family of convex functions: it is convex.

Finally, we demonstrate that $t \mapsto \min_{\lambda} g(t, \lambda)$ is convex. Observe that, for any fixed $\tau_i \geq 0$, the mapping

$$t \mapsto \sum_i \log(1 + \xi(a_i, t)\tau_i) - ts$$

is convex in t . Thus $\min_{\lambda} g(t, \lambda)$ is also the pointwise maximum of a family of convex functions: it is also convex. \square

Theorem. Fix $\alpha \in [0, 1]$. Let $a_i = |P_i|$. Let φ^* be given by Equation (2). Let $\mathcal{S}_k = \cup_{i=1}^k P_i$.

Let

$$\hat{s}(\mu) = \max \{s : \varphi_{\mathbf{a}, \mu}(s) \leq \alpha\}$$

and

$$\delta(s) = \max_{\mu: \varphi_{\mathbf{a}, \mu}(s) \geq \alpha} (\hat{s}(\mu) - \mu).$$

Let

$$U_k = \text{SDP}_{\mathcal{S}_k} + \frac{|\mathcal{S}_m|}{|\mathcal{S}_k|} (|\mathcal{S}_m| - \delta((1 - \text{SDP}_{\mathcal{S}_m})|\mathcal{S}_m|) - \text{SDP}_{\mathcal{S}_m}).$$

Then $\mathbb{P}(\text{SDR}_k \leq U_k \text{ for all } k) \geq 1 - \alpha$.

Proof. Let $S_k = \sum_{i=1}^k X_i$. We will first construct a simultaneous confidence interval on $\mu_k \triangleq \mathbb{E}[S_k]$; simultaneous confidence intervals on the corresponding SDRs will then be straightforward to obtain. Let

$$C(\mathbf{S}) = \{\hat{\boldsymbol{\mu}} : \hat{\mu}_k \geq S_k - \hat{s}(\hat{\boldsymbol{\mu}}_m) + \hat{\mu}_m \forall k\}.$$

a confidence region for $\boldsymbol{\mu}$. What is its coverage probability? Observing that $(S_1 - \mu_1, \dots, S_m - \mu_m)$ is a martingale and applying the submartingale inequality, we find that

$$\begin{aligned} \mathbb{P}(\boldsymbol{\mu} \notin C(\mathbf{S})) &= \mathbb{P}(S_k - \hat{\mu}_k > \hat{s}(\hat{\boldsymbol{\mu}}_m) - \hat{\mu}_m \forall k) \\ &\leq \inf_{t \geq 0} \mathbb{E}[\exp(t(S_m - \mu_m) - t(\hat{s}(\hat{\boldsymbol{\mu}}_m) - \hat{\mu}_m))] = \varphi_{\mathbf{a}, \mu_m}^*(\hat{s}(\hat{\boldsymbol{\mu}}_m)) \leq \alpha. \end{aligned}$$

Thus $C(\mathbf{S})$ is an α -valid confidence interval for μ_k .

The definition of C is unwieldy, as the bound on each parameter $\hat{\mu}_k$ is expressed in terms of a nontrivial function of the parameter $\hat{\mu}_m$. We can obtain a slightly larger confidence region by calculating an overall lower bound for each individual parameter. Letting

$$\begin{aligned}
\hat{\mu}_k^*(\mathcal{S}) &\triangleq \min_{\hat{\mu} \in C(\mathcal{S})} \hat{\mu}_k = S_k - \max_{\hat{\mu} \in C(\mathcal{S})} (\hat{s}(\hat{\mu}_m) - \hat{\mu}_m) \\
&= S_k - \max_{\hat{\mu}_m: \hat{\mu}_m \geq S_m - \hat{s}(\hat{\mu}_m) + \hat{\mu}_m} (\hat{s}(\hat{\mu}_m) - \hat{\mu}_m) \\
&= S_k - \max_{\hat{\mu}_m: \hat{s}(\hat{\mu}_m) \geq S_m} (\hat{s}(\hat{\mu}_m) - \hat{\mu}_m) \\
&= S_k - \max_{\hat{\mu}_m: \varphi_{\alpha, \mu}(\hat{s}) \geq \alpha} (\hat{s}(\hat{\mu}_m) - \hat{\mu}_m),
\end{aligned}$$

we are guaranteed that

$$\mathbb{P}(\hat{\mu}_k \geq \hat{\mu}_k^*(\mathcal{S}) \quad \forall k) \geq 1 - \alpha.$$

Finally, to calculate lower bounds on our objects of interest we recall that

$$\text{SDP}_{\mathcal{S}_k} = 1 - S_k / |\mathcal{S}_k|$$

$$\text{SDR}_{\mathcal{S}_k} = 1 - \hat{\mu}_k / |\mathcal{S}_k|.$$

Substituting these into the definition of $\hat{\mu}^*(\mathcal{S})$, we obtain our final result.

□

C Benjamini-Hochberg on L1000B data

The figure below visualizes the sorted p -values associated with the Gaussian model of the L1000B data.

D Merging confidence intervals

A confidence region generated by Theorem 4 produces an upper bound U_k for $\text{SDR}_{\mathcal{S}_k}$ for each subset \mathcal{S}_k . For large value of k these upper bounds can be quite close to the unbiased

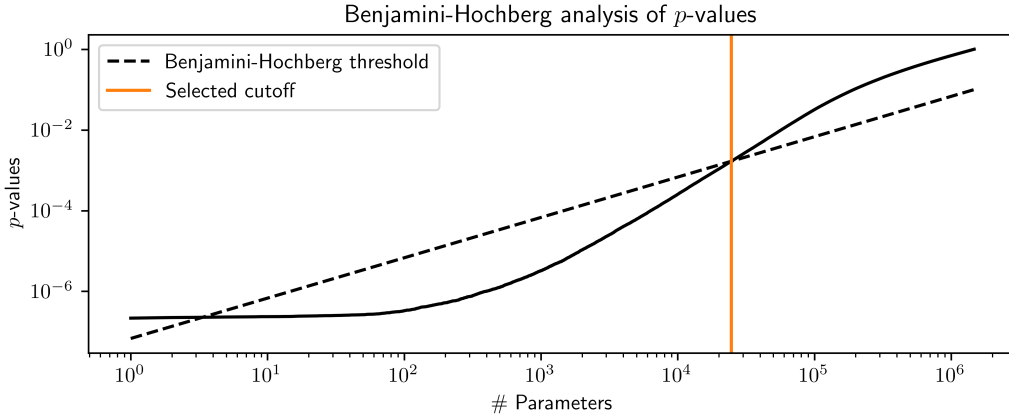


Figure 6: Benjamini-Hochberg with target error 10% makes 24629 discoveries. We plot the sorted p -values obtained from a Gaussian model on L1000B data against the Benjamini-Hochberg thresholds. The last point where the p -values lie below the corresponding thresholds occurs when considering 24629 parameters.

estimate of the SDR, i.e., the SDP. However, for small values of k these upper bounds can be quite large.

It is possible to obtain smaller confidence regions by merging a collection of confidence regions generated from Theorem 4. Specifically, we choose four thresholds by uniformly spacing five values between the minimum observed confidence score and the maximum observed confidence score and discarding the last value. For each threshold, we discard parameters whose confidence scores are below the threshold and construct a simultaneous $(1 - \alpha/4)$ confidence region using Theorem 4. The intersection of the four regions then constitutes a simultaneous $(1 - \alpha)$ confidence region.